



Temperature Dependent Properties of Pd-GaN Thin Film Grown by a Low-cost Electrochemical Deposition Technique

k.al-heuseen

Al-Balqa' Applied University, Ajloun University College, Jordan.

ARTICLE INFO

Article history:

Received: 9 September 2016;

Received in revised form:
25 October 2016;

Accepted: 3 November 2016;

Keywords

Pd-GaN Schottky diodes,
thermionic emission,
Gaussian distribution,
Electrical properties.

ABSTRACT

A Schottky barrier on GaN film grown on Si (111) substrate by low cost electrochemical deposition technique at 20 °C was obtained and characterized. Pd was used as a Schottky barrier contact. The temperature dependent current-voltage (*I-V-T*) curves have been measured on Pd/GaN contacts in the range of 300-470 K. Thermionic emission theory has been applied to the curves and the Schottky barrier heights, ϕ_{B0} , and ideality factors, n , have been calculated. Barrier heights and ideality factors are evaluated as functions of temperature. These measurements indicate that the Schottky barrier height increases and ideality factor decreases with increasing temperature. The apparent Richardson constant was found to be $2.38 \times 10^{-7} \text{ Acm}^{-2} \text{ K}^{-2}$ and mean barrier height of 0.3 eV. After barrier height inhomogeneities correction, by assuming a Gaussian distribution (GD) of the barrier heights, the Richardson constant and the mean barrier height were obtained as $19.3 \text{ Acm}^{-2} \text{ K}^{-2}$ and 1.54 eV, respectively. The corrected Richardson constant was very closer to theoretical value of $26 \text{ Acm}^{-2} \text{ K}^{-2}$.

© 2016 Elixir All rights reserved.

Introduction

GaN is a wide direct band gap semiconductor, which has a broad range of electrical applications especially, in high temperature electronic devices, optoelectronic and high-power devices [1]. In recent years, many efforts have been made to grow GaN thin films by various growth techniques, including metalorganic chemical vapor deposition (MOCVD) [2], reactive molecular beam epitaxy (MBE) [3], hydride vapor phase epitaxy (HVPE) [4] and reactive sputtering [5]. However, these are very expensive techniques, which added to the high cost of the products made from such material. The search for cost effective technique therefore has began and seems to have found hopes in chemical related technique, namely electrochemical deposition (ECD) [6,7]. The advantages of the ECD in comparison with other methods are as follows: the thickness and surface morphology can be controlled by growth parameters, the deposition rate is relatively high, the experimental setup is low-cost, process temperature is low, and ease of impurity doping. However, the growth of GaN thin films is still a big challenge. Up to now there are only a few theoretical and experimental studies on ECD of GaN [6, 7].

To construct GaN optoelectronic and high-power devices, it is necessary first to clarify the physics of metal/GaN interface and its influence on electrical characteristics of metal/GaN Schottky diodes. Metals such as Pt ($\phi_m = 5.65$ eV), Ni ($\phi_m = 5.15$ eV), Pd ($\phi_m = 5.12$ eV) and Au ($\phi_m = 5.1$ eV) are commonly used for Schottky contact processing [8-11]. In addition, the application of GaN devices at high temperatures requires a full understanding of the thermal behavior of contacts and the relevant degradation mechanisms. The Schottky barrier measured only at room temperature does not give detailed information about the conduction process and the nature of barrier formed at the metal/GaN interface.

A lot of work has already been reported on electrical characterization but there are few works studied the temperature dependence of electrical characteristics of GaN Schottky diodes. Akkal *et al* [12] investigated the current-voltage characteristics of Au/n-GaN Schottky diodes below room temperature in the range 80-300 K. Osvald *et al* [10] investigated the temperature dependence of the electrical characteristics of GaN Schottky diodes with two crystal polarities (Ga- and N-face). They reported a decrease in the barrier height with a decrease in temperature and an increase in ideality factor for both polarities. Arehart *et al* [13] studied the impact of threading dislocation density on the Ni/n-GaN Schottky diode using forward measurements. Tekeli *et al* [14] investigated the behavior of the forward bias (*I-V-T*) characteristics of inhomogeneous (Ni/Au) - $\text{Al}_{0.3}\text{Ga}_{0.7}\text{N}/\text{AlN}/\text{GaN}$ heterostructures in the temperature range of 295–415 K using double layers of metal and multi layers of GaN and AlN. Recently, Ravinandan *et al* [15] reported on the temperature-dependent electrical characteristics of the Au/Pd/n-GaN Schottky diode in the temperature range of 90–410 K..

In this work, we study electron transport through Pd metal Schottky contact on GaN thin film on Si (111) substrate. Our GaN films were deposited on Si using a low cost electrochemical technique. The electrical properties of the Schottky contact were measured from 300 to 470 K. A wide range of temperature well above room temperature is very important in order to get more accurate results on single metal Schottky contact on an electrochemically deposited GaN film. The values of ideality factor (n), barrier height (ϕ_{B0}) and series resistance (R_s) were extracted from the forward bias *I-V* measurements. The temperature dependence of the Schottky barrier height of Pd/GaN are interpreted based on the existence of the Gaussian distribution (GD) of the barrier

heights around a mean value due to the barrier height inhomogeneities prevailing at the metal-semiconductor interface.

Experimental procedure

GaN thin film was prepared on n-type Si (111) substrate by ECD technique using a mixture of gallium nitrate ($\text{Ga}(\text{NO}_3)_3$) with ammonium nitrate (NH_4NO_3) (ratio 1:1 by weight) in 10ml deionized water at 20°C (Ga melting point at 29°C) [6, 7]. Using a simple two-electrode homemade Teflon cell, a gallium plate with (99.999%) purity was used as an anode and the substrates as cathode. The distance between the electrodes was about 0.5 cm. A constant electrodeposition current density of $2.5\text{mA}/\text{cm}^2$ was applied for 12 h. After GaN film was synthesized, the diode was completed by deposition of Pd on a portion of the sample of n-GaN using the A500 Edwards RF magnetron sputtering unit. The ultimate pressure was 1×10^{-6} mbar, which was raised to 2×10^{-2} mbar by purging the chamber with high purity argon gas (Ar 99.99%); the power of sputtering was 150W. Our metal-semiconductor-metal (MSM) diodes with both interdigitated contacts (electrodes) forming Schottky barriers. The fingers width is $230\ \mu\text{m}$ and the finger spacing is $400\ \mu\text{m}$. The length of each electrode is about 3.3 mm, and it consists of four fingers at each electrode. The (*I-V*) measurements of the sample were carried out using the Keithley model 2400 on different temperature in the range 300-470K. The operation temperature of the diodes was measured by a calibrated K-type thermocouple mounted on the device.

Results and discussion

Fig. 1 shows SEM image and EDX spectrum of GaN thin film deposited on Si (111). The film was deposited using a constant current density $2.5\ \text{mA}/\text{cm}^2$ for 12 h. The surface morphology of the GaN thin film shows a network of nano-flake structures. The EDX analysis shows the presence of GaN and possibly Ga_2O_3 .

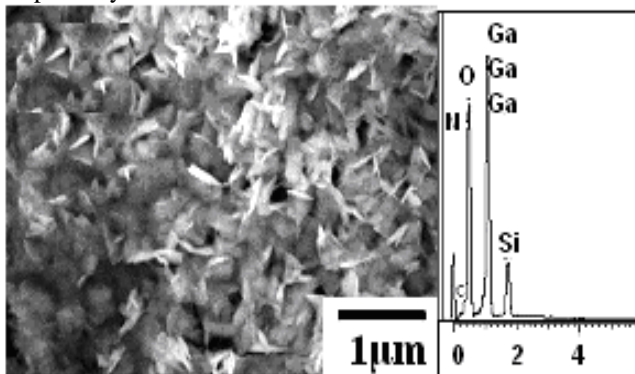


Figure 1. SEM micrograph and EDX spectra of GaN thin film deposited on Si (111) by constant current density $2.5\text{mA}/\text{cm}^2$ for 12h.

Fig. 2 shows the typical XRD pattern of GaN film deposited on Si (111) by ECD technique. The XRD spectra indicated two peaks; one at $2\theta = 32.9^\circ$ and the other at $2\theta = 40.1^\circ$ for c-GaN corresponding to reflections from (100) and (002) planes respectively. A small peak could be observed at $2\theta = 34.5^\circ$ for h-GaN corresponding to reflections from (0002) plane. A strong peak at $2\theta = 58.9^\circ$ for h-GaN corresponds to reflection from (110) plane [16]. A peak with weak intensity of $\beta\text{-Ga}_2\text{O}_3$ could be observed at $2\theta = 37.8^\circ$ corresponding to reflection plane (11-3). There are two other strong peaks at $2\theta = 28.4^\circ$ and $2\theta = 58.8^\circ$ corresponding to Si (111) and Si (222) respectively. Thus, the film deposited here contains both the hexagonal and cubic phases of GaN. From the XRD data, the

determined lattice constants are $a=3.35\ \text{\AA}$, and $c=5.159\ \text{\AA}$ for hexagonal, which are in good agreement with reported values [17, 18]. The average size of h-GaN crystals, *D* calculated from the well known Scherrer formula is between 18 and 19 nm.

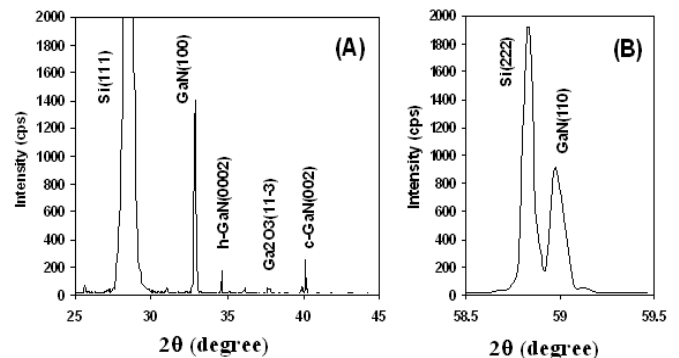


Figure 2. XRD of deposited GaN films on Si (111) using constant current density $2.5\ \text{mA}/\text{cm}^2$ for 12h, A) for the range of $2\theta=25\text{-}45^\circ$, B) for the range of $2\theta=58.5\text{-}59.5^\circ$.

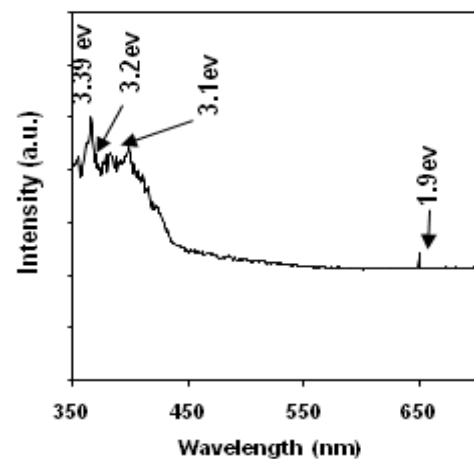


Figure 3. PL spectra of deposited GaN films on Si (111) for 12h using constant current density $2.5\ \text{mA}/\text{cm}^2$.

Fig. 3 shows the PL spectrum of GaN/Si(111) recorded at room temperature. Four peaks at 3.39, 3.2, 3.1 and 1.9 eV can be observed on the PL spectra. The peak positions at 3.39 and 3.2 eV are due to the band gap for h-GaN and c-GaN respectively, and these values are in good agreement with other reported works [19, 20]. The third peak centered at 3.1 eV, may be due to the donor acceptor (DA) transition [21]. The last observed peak centered at 1.9 eV has low intensity and may be due to the deep level states related to gallium or nitrogen vacancy [22].

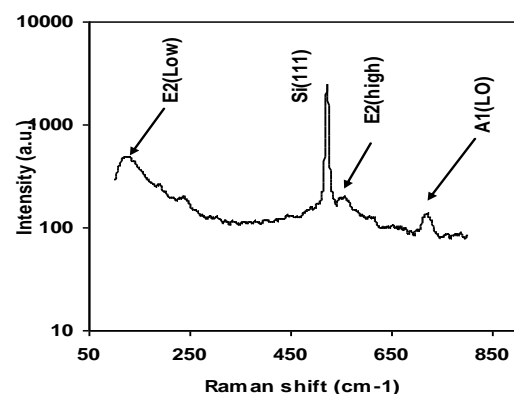


Figure 4. Raman spectra of GaN deposited on Si (111) for 12h and current density $2.5\ \text{mA}/\text{cm}^2$.

Fig. 4 shows a room temperature micro-Raman spectrum of GaN deposited on Si (111) for 12h and current density 2.5 mA/cm². A strong band is observed at 522.04 cm⁻¹, which is the contribution from the Si (111) substrate, and a small band at 250cm⁻¹, may be due to the acoustic phonons of Si. Three Raman active optical phonons have been clearly assigned to GaN, one for c-GaN at 733 cm⁻¹ due to A₁ (LO) modes, and two modes for h-GaN at 140 cm⁻¹ and 566cm⁻¹ due to E₂(Low) and E₂(high) respectively [23].

Fig. 5a shows typical temperature dependent current-voltage (*I-V*) characteristics of the Pd/GaN Schottky diode measured in atmospheric conditions, at different temperatures in the range from (300–470K) and recorded from -5 to 5 V. The curves obtained for the *I-V* measurements indicate a very strong temperature dependence of the Pd/GaN Schottky diodes. In addition, the current increases with increasing temperature for both forward and reverse biases. From this figure, one can observe that the contact of Pd with a GaN acts as rectifying junction in forward and reverse currents. The figure also showed an increment of the linear region as the temperature increases. Fig. 5b shows series resistance of the current versus operating temperature showing decreasing value as temperature increases and tend towards constant value at high temperatures. In another words the linear region shows an increase with increasing operating temperature indicating more thermionic transport mechanism involved at higher temperature.

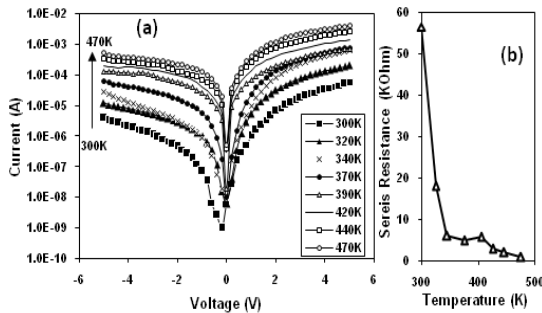


Figure 5 a. Temperature dependent *I-V* plot of the Pd/GaN Schottky diode in the temperature range (300–470K) and b) Series resistance versus operating temperature.

The forward *I-V* characteristics were analyzed using standard thermionic emission relation for electron transport from a metal-semiconductor with low doping concentration. It is given by the following equation when higher values of $V > 3kT/q$ [24, 25]

$$I = I_0 \exp\left[\frac{qV - IR_s}{nKT}\right] \quad (1)$$

and the saturation current I_0 is given by

$$I_0 = AA^{**}T^2 \exp\left[\frac{-q\phi_B}{kT}\right] \quad (2)$$

where V is the voltage across the diode, n the ideality factor, k is the Boltzman constant, q is the electron charge, T is the temperature, A is the contact area, A^{**} is the effective Richardson constant and ϕ_{B0} is the Schottky barrier height. By plotting $\ln(I)$ vs. V for each temperature in the range (300–470K) for the Pd/GaN Schottky diode we get a straight line with the slope = q/nkT and y-intercept ($V=0$) at $\ln I_0$. From the value of I_0 , Schottky barrier height ϕ_{B0} was calculated using Eq. 2. In addition, from the slope the ideality factor was calculated, which is a measure of the thermionic emission

current transport ideality. Fig. 6 shows the ideality factor and the barrier height as a function of temperature in the temperature range (300–470K) for the Pd/GaN Schottky diode.

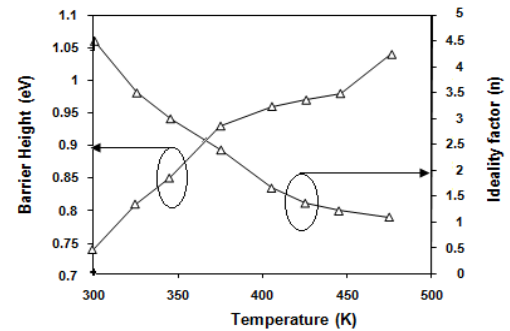


Figure 6. Barrier heights and ideality factors as a function of temperature in the temperature range (300–470K) for the as-deposited Pd/GaN Schottky diode.

One can observe that the ideality factor n decreases with increasing temperature while the Schottky barrier height increases with temperature. A similar observation was noted by Ravinandan *et al* [18] in Pd/Au/GaN. The ideality factor decreased from 4.5 at 300K and approaches unity and becomes stable over 400K. Thus, the thermionic emission model is dominating at temperature over 400K. The large value of n at room temperature suggests the presence of an interfacial native oxide layer between Pd and GaN and this layer was reduced as the temperature increased. According to [15,26] the existence of Schottky barrier height inhomogeneity was often used to explain such a temperature dependence of ϕ_{B0} and n . Assuming that a diode consists of parallel segments of different barrier heights and each contributes to the current independently (parallel conduction model), the current of the diode will preferentially flows through the lower barriers. As a result, the current conduction is dominated by patches of lower barrier height with a large ideality factor at lower temperatures. However, as the temperature increases, an increasing number of electrons will have sufficient energy to surmount the higher barriers; consequently, the dominant barrier height will increase with increasing both temperature and bias voltage. Thus, both the barrier height and ideality factor observed from the temperature-dependent characteristics are consistent with barrier height inhomogeneity [26]. In addition, these observations are in a good agreement with other reported works and with the thermionic emission theory [27].

Equation (2) can also be used to construct a Richardson plot of $\ln(I_0/AT^2)$ versus $1/kT$, with the slope giving ϕ_{B0} and A^{**} determined by the intercept. This plot is shown in Fig. 7.

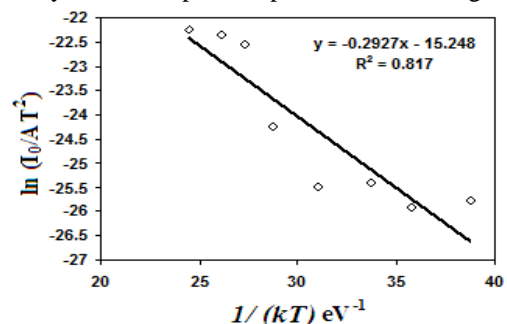


Figure 7. Richardson plot, $\ln(I_0/AT^2)$ versus $1/(kT)$, for the Pd/GaN in the temperature range (300–470K) for the Pd/GaN Schottky diode.

From the linear fit in the $\ln(I_0/AT^2)$ versus $1/kT$ plot, as shown in Fig. 7, Richardson constant and Schottky barrier heights values were $2.38 \times 10^{-7} \text{Acm}^{-2}\text{K}^{-2}$ and 0.3 respectively. This deviation in A^{**} from the theoretical value ($26 \text{Acm}^{-2}\text{K}^{-2}$) is a general case for most of the Schottky diodes given in the literature for different materials [28, 29]. This deviation is generally explained by the barrier inhomogeneity of the contact, which means that it consists of high and low barrier areas at the interface mainly due to the formation of different oxides layer thickness between the metal and semiconductors. In addition, the effective area for current conduction (A_{eff}) is significantly lower than the geometric contact area (A_{geom}) due to preferential current flow through lower barrier height regions [30, 31].

In order to explain the abnormal behavior between the theoretical and experimental values of Richardson constant, let us assume that the distribution of the barrier heights is a Gaussian distribution of barrier heights with a mean value φ_B and standard deviation σ_s , which can be given by [32-34]

$$P(\varphi_B) = \frac{1}{\sigma_s \sqrt{2\pi}} \exp\left[-\frac{(\varphi_B - \bar{\varphi}_B)^2}{2\sigma_s^2}\right] \quad (3)$$

where $1/(\sigma_s \sqrt{2\pi})$ is the normalization constant of the Gaussian barrier height distribution. The total current I (V) across a Schottky diode containing barrier inhomogeneities can be expressed as [35]

$$I(V) = \int_{-\infty}^{+\infty} I(\varphi_B, V) P(\varphi_B) d\varphi \quad (4)$$

Where $I(\varphi_B, V)$ is the current at a bias V for a barrier of height based on the ideal thermionic emission diffusion theory and $P(\varphi_B)$ is the normalized distribution function giving the probability of accuracy for barrier height. Performing this integration, one can obtain the current $I(V)$ through a schottky barrier at a forward bias but with a modified barrier as

$$I(V) = I_0 \exp\left(\frac{qV}{n_{ap}kT}\right) [1 - \exp\left(-\frac{qV}{kT}\right)] \quad (5)$$

with

$$I_0 = AA^{**} T^2 \exp\left(\frac{q\varphi_{ap}}{kT}\right) \quad (6)$$

Where φ_{ap} and n_{ap} are the apparent barrier height at zero bias and apparent ideality factor, respectively, and given by [33, 36]

$$\varphi_{ap} = \varphi_B(T=0) - \frac{q\sigma_{s0}^2}{2kT} \quad (7)$$

$$\left(\frac{1}{n_{ap}} - 1\right) = \rho_2 - \frac{q\rho_3}{2kT} \quad (8)$$

We need to assume that the mean Schottky barrier height φ_{B0} and σ_s are linearly bias-dependent on Gaussian parameters, such that $\varphi_B = \varphi_{B0(T=0)} + \rho_2 V$ and standard deviation $\sigma_s = \sigma_{s0} + \rho_3 V$, where ρ_2 and ρ_3 are voltage coefficients which may depend on temperature, quantifying the voltage deformation of the barrier height distribution [37]. The temperature dependence of σ_s is small and therefore can be neglected [38].

We attempted to draw a φ_B versus $q/2kT$ plot (Fig.8) to obtain evidence of the GD of the barrier heights and from the intercept and the slope the value of φ_{B0} is 1.52eV and the value

of σ_{s0} is 0.199, respectively. The structure with the best rectifying performance presents the best barrier homogeneity with the lower value of the standard deviation. It was seen that the value of σ_{s0} is not small compared to the mean value values of φ_{B0} , and it indicates the presence of the interface inhomogeneities. Therefore, the plot of $[1/(n)-1]$ versus $q/2kT$ should be a straight line that gives the voltage coefficients $\rho_2 = 1.097 \text{ V}$ and $\rho_3 = 0.101 \text{ V}$ from the intercept and the slope, respectively (Fig.8).

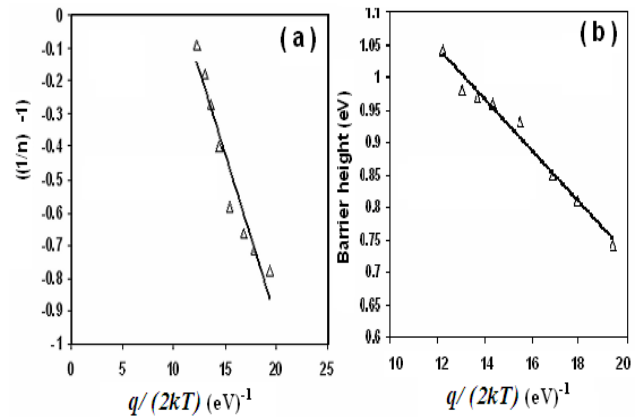


Figure 8. Ideality factor (a) and apparent barrier height (b) versus $q/(2kT)$ curves of the Pd/GaN/Si(111) Schottky diode according to the Gaussian distribution of the barrier heights.

Now, by combining Eqs. (6) and (7), the Richardson plot can be modified to

$$\ln\left(\frac{I_0}{T^2}\right) - \frac{q^2 \sigma_{s0}^2}{2k^2 T^2} = \ln(AA^{**}) - \frac{q\varphi_{B0}}{kT} \quad (9)$$

Fig. 9 shows the modified $\ln(I_0/T^2) - q^2 \sigma_{s0}^2 / 2k^2 T^2$ versus $1/kT$ plot. By the least squares linear fitting of the data $\varphi_{B0} = 1.54 \text{eV}$ and $A^{**} = 19.3 \text{A/cm}^2 \text{K}^2$ are obtained. As can be seen, $\varphi_{B0} = 1.54 \text{eV}$ from this plot according to Eq. (12), is in good agreement with the value of $\varphi_{B0} = 1.52 \text{eV}$ from φ_B versus q/kT (Fig.8) and the value of Richardson constant are very close to the theoretical value of $26 \text{Acm}^{-2}\text{K}^{-2}$. Therefore, it can be concluded that the temperature dependence of the forward $I-V$ characteristics of the Pd on the electrochemically deposited GaN films can be successfully explained based on the thermionic emission mechanism with a Gaussian distribution of the barrier heights.

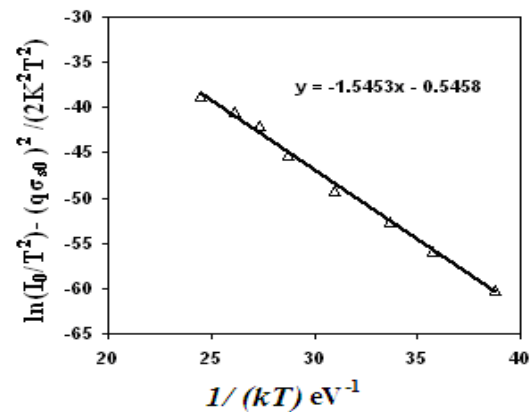


Figure 9. Modified Richardson plot for the Pd/GaN/Si(111) Schottky diode according to the Gaussian distribution of barrier heights.

Conclusions

The GaN thin film has been successfully grown on Si (111) using ECD technique. Using this film, Pd/GaN Schottky barrier diode was fabricated and its forward bias I - V characteristics were studied in the temperature range of 300-470K. The Schottky barrier height, ideality factor, saturation current and series resistance of the device characteristics have been found to be strongly dependent on the operating temperature, which could be partly attributed to the inhomogeneities at the metal-semiconductor interface. The barrier height increases and the ideality factor decreases with increasing temperature which indicated that the diode are dominated by thermionic emission at high temperatures than at low temperatures. The inhomogeneities can be described by the Gaussian distribution of the barrier heights with mean barrier height ϕ_{B0} is 1.52eV and standard deviation σ_{s_0} is 0.199. After Gaussian distribution correction the mean barrier height and the Richardson constant values obtained were 1.54eV and 19.3 A/cm² K², respectively, by means of the modified Richardson plot. This value of Richardson constant is in closed agreement with the theoretical value of 26.4 A/cm² K² of electrons in n-GaN. This work showed that the current transport mechanisms through Pd metal on electrochemically deposited GaN films is the same as those on epitaxial c-GaN grown by more highly sophisticated growth techniques.

References

- [1] R. V. Rajagopal, R. P. Koteswara, C.K. Ramesh. 2007 *Materials Science and Engineering B* 137 200–204.
- [2] H. Amano, T. Tanaka, Y. Kunii, K. Kato, S.T. Kim, and I. Akasaki, *J. Appl. Phys. Lett.* Vol. 64, pp. 1377–1379, 1994.
- [3] S.A. Nikishin, N.N. Faleev, V.G. Antipov, S. Francoeur, L. Grave de Peralta, G.A. Seryogin, H. Temkin, T.I. Prokofyeva, M. Holtz, S.N.G. Chu, *J. Appl. Phys. Lett.* 75 (1999) 2073–2075.
- [4] J. Jasinski, W. Swider, Z. Liliental-Weber, P. Visconti, K.M. Jones, M.A. Reshchikov, F. Yun, H. Morkoc- , S.S. Park, K.Y. Lee, *J. Appl. Phys. Lett.* Vol. 78, pp. 2297–2299, 2001.
- [5] E. Nahlah, R.S. Srinivasa, S. Major, S.C. Sabharwal, K.P. Muthe, *J. Thin Solid Films.* Vol. 333, pp. 9–12, 1998.
- [6] R.K. Roy, A.K. Pal, *Mater. Lett.* Vol. 59, pp. 2204–2209, 2005.
- [7] K. Al-Heuseen, M.R. Hashim, N.K. Ali, *Mater. Lett.* Vol. 64, pp. 1604–1606, 2010.
- [8] Q. Z. Liu, L. S. Yu, S. S. Lau, J. M. Redwing, N. R. Perkins and T. F. Kuoch. *Appl. Phys. Lett.* Vol. 70, pp. 1275, 1997.
- [9] C.K. Tan, A. Abdul Aziz, and F. K. Yam, *Applied Surface Science* , Vol. 252, pp. 5930–5935, 2006.
- [10] J. Osvald, J. Kuzmik, G. Konstantinidis, P. Lobotka and A. Georgakilas, *Microelectronic Engineering* , Vol. 81. Pp. 181-187, 2005.
- [11] Mehmet Ali Ebeoglu, *Physica B.* Vol. 403, pp 61–66, 2008.
- [12] B. Akkal, Z. Benamara, H. Abid, A. Talbi and B. Gruzza, *Materials Chemistry and Physics.* Vol. 85 pp. 27, 2004.
- [13] A. R. Arehart, B. Moran, J. S. Speck, U. K. Mishra, S. P. Den Baars, and S. A. Ringel, *J. Appl. Phys.* Vol.100, pp. 023709, 2006.
- [14] Z. Tekeli, Ş. Altındal, M. Çakmak and S. Özçelik, *J. Appl. Phys.* Vol. 102, pp. 054510, 2007.
- [15] M. Ravinandan, R. P. Koteswara and R.V. Rajagopal *Semicond. Sci. Technol.* Vol. 24, pp. 035004, 2009.
- [16] S. Strite and H. Morkoc, *J Vac Sci Technol.* Vol. B10, pp. 1237, 1992.
- [17] T. Detchprohm, K. Hiramatsu, K. Itoh and I. Akasaki, *Jpn J Appl Phys*, Vol. 31, pp. L1454-56, 1992.
- [18] T. Barfels, H.J. Fitting, J. Jansons, I. Tale, A. Veispals, A. Czarnowski von and H. J. Wulff, *Appl Surf Sci*, Vol. 179, pp. 191-195, 2001.
- [19] H. Zhang, Z. Ye and B. Zhao, *J Appl Phys*, Vol. 87, pp. 2830-34, 2000.
- [20] L. Wang, X. Liu, Y. Zan, J. Wang, D. Lu and Z. Wang, *Appl Phys Lett*, Vol. 72, pp. 109-111, 1998.
- [21] B. Deb, S. Chaudhuri and A.K. Pal, *Materials Letters* Vol.53, pp. 68– 75, 2002.
- [22] S.J. Rhee, S. Kim, E.E. Reuter, S.G. Bishop, R.J. Molnar. *Appl Phys Let*, Vol.73, pp. 2636-38, 1998.
- [23] Jian Zi, Guanghong Wei, Kaiming Zhang and Xide Xie. *J Phys Condensed Matter* , Vol. 8, pp. 6329-36,1996.
- [24] E. H. Rhoderick and R. H. Williams, *Metal Semiconductor Contacts 2nd edn*(Oxford: Oxford University Press), 1988.
- [25] V. L. Rideout, *Solid-State Electron.* Vol. 18, pp. 541-545, 1975.
- [26] S. Karadeniz, M. Sahin, N. Tugluoglu and H. Safak 2004 *Semicond. Sci. Technol.* Vol. 19, pp. 1098, 2004.
- [27] L. Fei, Z. Xiao-Ling, D. Yi, X. Xue-Song and Chang-Zhi Chinese physics B, Vol. 18, pp. 5029-33,2009.
- [28] Ş. Altındal, H. Kanbur, D. E. Yıldız, and M. Parlak, *Appl. Surf. Sci.* Vol. 253, pp. 5056, 2007.
- [29] B .M. Green, K. K. Chu, E. M. Chumbes, J. A. Smart, J. M. Shealy and L.F. Eastman, *I EEE Electron Device Lett.* Vol.21, pp. 268, 2000.
- [30] F. Lucolano, F. Roccaforte, F. Giannazzo, V. Raineri, J. Appl. Phys. Vol. 102, pp. 113 701, 2007.
- [31] F. Roccaforte, F. La Via, V. Raineri, R. Pierobon, E. Zanoni, *J. Appl. Phys.* Vol. 93 ,pp. 9137–9144, 2003.
- [32] S. Altındal, S. Karadeniz, N. Tougluoglu, A. Tataroglu, *Solid-State Electron.* Vol. 47, pp. 1847, 2003.
- [33] J. H. Werner, H.H. Guttler, *J. Appl. Phys.* Vol. 69, pp. 1522, 1991.
- [34] Y.P.Song, R.L.Meirhaeghe, W.H.Laflere, F.Cardon, *Solid State Electron*, Vol. 29, pp. 663, 1986.
- [35] I. Dokme, S. Altındal, M.M. Bulbul, 2006 *Appl. Surf. Sci.* 252 7749.
- [36] S. Zeyrek, S. Altındal, H. Yüzer, M. M. Bülbül, *Appl. Surf. Sci.* Vol. 252, pp. 2999, 2006.
- [37] S. Zhu, R. L. VanMeirhaege, C. Detavernier, F. Cardon, G. P. Ru, X. P. Qu, B. Z. Li, *Solid State Electron*, Vol. 44, pp. 663, 2000.
- [38] M. K. Hudait, S. P. Venkateswarlu, S. B. Krupanidhi, *Solid State Electron.* Vol. 45, pp. 133, 2001.